Universitat Politècnica de Catalunya

Physics Engineering final project

Diagrammatic expansions of Hubbard models

Author:
Juan Manuel Losada

Advisor:
Ferran Mazzanti Castrillejo

June 19, 2016

Contents

Introduction

Optical lattice are periodic structures made of light, they are formed by the interference of laser beams producing standing waves ([6]). When three standing waves in different directions superpose, a crystal-like potential is created, and atoms will fall in the potential minima. The depth and the periodicity of the optical lattice can be highly controlled, therefore, optical lattices provide an ideal framework to study quantum effects. In this work we will compute some relevant quantities of a system of electrons on an optical lattice using Feynman Diagrams.

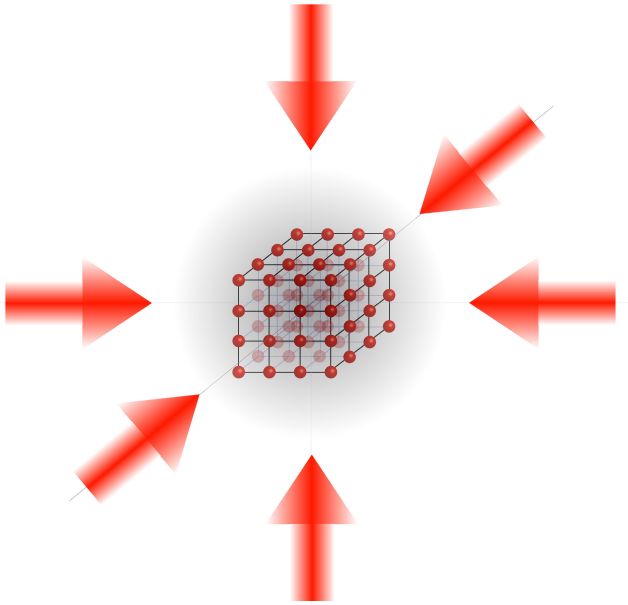

Figure 1: An optical lattice is created by standing waved inside a cavity

The aim of this work is to learn this extremely powerful technique. Perturbative analysis based on Feynman diagrams is a extensively used used tool in theoretical physics, and it becomes essential in some many-body problems. In order to develop diagrammatic expansion we will have to understand first some preliminaries: second quantization, perturbative theory and Green's function formalism.

We will apply this tools to the case of an optical lattice. To do that, first we will solve the single particle problem of an electron on an optical lattice. Then, we will use the obtained basis of eigenfunctions to compute the energy corrections to these eigenstates when interaction between particles is switched on. The energy correction will be computed using three different well-known diagrammatic expansions: Hartree-Fock, random phase approximation (RPA) and the ladder expansion.

Three different of interactions between particles will be studied for $V(x_i, x_j) = V(|x_i - x_j|)$:

1. A delta potential $V(x) = V_{int}\delta(x)$
2. A soft sphere potential:
$$V(x) = \begin{cases} V_{int}, \text{ for, } |x| < r_0 \\ 0, \text{ elsewhere} \end{cases}$$
3. A Colagero-Sutherland potential:
$$V(x) = V_{int} \frac{\pi^2/L^2}{\sin\left(\frac{\pi}{L}x\right)^2} \tag{1}$$

The delta potential and the soft sphere potential are well-known toy potentials. The Calogero-Sutherland potential describes a system of particles in a ring with a Coulomb-type interaction. The interest of this potential is its exact solvability in the many-body problem ([9]). In the three potential we will treat V_{int} as the coupling constant.

Second quantization

Throughout this work we will extensively make use of the second quantization formalism. In this chapter we will present the notation used for fermionic systems, but we will not explain second quantization in detail (see, for example, [1], [2] and [3]).
Firstly, consider a system of N fermions in the single-particle states $\alpha_1, \ldots, \alpha_N$. The wavefunction of this system is a Slater determinant:

$$\begin{aligned}\Phi(x_1, \ldots, x_N) &= \frac{1}{\sqrt{N!}} \sum_{P \in S_N} sgn(P) \phi_{\alpha_{P(1)}}(x_1) \cdots \phi_{\alpha_{P(N)}}(x_N) \\ &= \frac{1}{\sqrt{N!}} \begin{vmatrix} \phi_{\alpha_1}(x_1) & \cdots & \phi_{\alpha_1}(x_N) \\ \vdots & & \vdots \\ \phi_{\alpha_N}(x_1) & \cdots & \phi_{\alpha_N}(x_N) \end{vmatrix}\end{aligned} \tag{1.1}$$

Where $\phi_{\alpha_k}(x)$ is the single particle wavefunction of a fermion in state α_k. Observe that if two fermions were in the same state, the determinant would vanish.
Now, we will denote the fermion annihilation and creators operator of a state α_k as $\hat{c_{\alpha_k}}$ and $\hat{c}^\dagger_{\alpha_k}$, respectively. $\hat{c_{\alpha_k}}$ transforms a wavefunction of N fermions, one of which is in state α_k into a wavefunction of $N-1$ fermions by eliminating it. If no fermion is in state α_k in the original wavefunction, acting with $\hat{c_{\alpha_k}}$ gives 0. $\hat{c}^\dagger_{\alpha_k}$ creates a fermion in state α_k instead of removing it. A very important property about these operators is their anticommutation relations:

$$\begin{aligned}\{\hat{c}^\dagger_k, \hat{c}_l\} &= \delta_{k,l} \\ \{\hat{c}_k, \hat{c}_l\} &= 0 \\ \{\hat{c}^\dagger_k, \hat{c}^\dagger_l\} &= 0\end{aligned} \tag{1.2}$$

Also, $\hat{n}_k = \hat{c}^\dagger_k \hat{c}_k$ is the number operator, and if acting on a wavefunction if gives the number of fermions in state α_k.
Any other operator in the Fock space can be written in terms of $\hat{c_k}$ and $\hat{c}^\dagger_k$, for instance, the Hamiltonian written in the second quantization formalism is:

$$\hat{H} = \sum_{i,j} \hat{c}^\dagger_i \langle i| T |j\rangle \hat{c}_j + \frac{1}{2} \sum_{i,j,k,l} \hat{c}^\dagger_i \hat{c}^\dagger_j \langle ij| V |kl\rangle \hat{c}_l \hat{c}_k \tag{1.3}$$

When working on the interaction picture (also known as Dirac picture) the creation and annihilation operators have a very simple form which we will not prove:

$$\hat{c}_j(t)_I = \hat{c}_j e^{-\frac{i}{\hbar}\epsilon_j t}$$
$$\hat{c}_j^\dagger(t)_I = \hat{c}_j^\dagger e^{\frac{i}{\hbar}\epsilon_j t}$$

Now we are ready to state the Hubbard model.

Hubbard model

The Hubbard model is a simple model describing interacting fermions on a lattice. This model is an extension of the thigh binding model including short range interactions. The Hubbard Hamiltonian is written as:

$$H = -t \sum_{\langle i,j\rangle\sigma} \hat{c}^\dagger_{j\sigma}\hat{c}_{i\sigma} + U\sum_i n_{i\uparrow}n_{i\downarrow}, \tag{2.1}$$

where $\hat{c}^\dagger_{j\sigma}$ is the creation operator of a fermion in site j and σ denotes the spin state. $\langle i,j\rangle$ implies adjacent sites and t and U are parameters which depend on the optical lattice and on the fermions (there exists a correspondence between the first quantization problem in the optical lattice and the t and U parameters of the second quantization model).

The first term is known as the "hopping term", and it is the same appearing in the tight binding approximation. The second term is the on-site interaction, it only contributes when $n_{i\uparrow} = 1$ and $n_{i\downarrow} = 1$, when there are two electrons in the same site. This corresponds to a contact interaction between particles with different spin.

If now we go to the reciprocal basis, $\hat{c}_{j\sigma} = \frac{1}{\sqrt{N}}\sum_k e^{ijk}\hat{c}^\dagger_{k\sigma}$, we have, for the hopping term:

$$\begin{aligned} -t\sum_{\langle l,j\rangle\sigma}\hat{c}^\dagger_{j\sigma}\hat{c}_{l\sigma} &= -\frac{t}{N}\sum_{\langle l,j\rangle}\sum_{k,k'} e^{ijk}e^{-ilk'}\hat{c}^\dagger_{k\sigma}\hat{c}_{k'\sigma} = -\frac{t}{N}\sum_{k,k',\sigma}\hat{c}^\dagger_{k\sigma}\hat{c}_{k'\sigma}\sum_j (e^{ijk}e^{-i(j-1)k'} + e^{ijk}e^{-i(j+1)k'}) = \\ &= -\frac{t}{N}\sum_{k,k',\sigma}\hat{c}^\dagger_{k\sigma}\hat{c}_{k'\sigma}(e^{ik'} + e^{-ik'})\sum_j e^{ij(k-k')} = -t\sum_{k,k',\sigma}\hat{c}^\dagger_{k\sigma}\hat{c}_{k'\sigma}2\cos(k')\delta_{k,k'} = \sum_{k,\sigma}\epsilon_k n_{k,\sigma} \end{aligned} \tag{2.2}$$

With $\epsilon_k = -2t\cos(k)$. For the on-site interaction term we have:

$$\begin{aligned} U\sum_l n_{l,\uparrow}n_{l,\downarrow} &= U\sum_l \hat{c}^\dagger_{l,\uparrow}\hat{c}_{l,\uparrow}\hat{c}^\dagger_{l,\downarrow}\hat{c}_{l,\downarrow} = \frac{U}{N^2}\sum_{k_1,k_2,k_3,k_4}\sum_l \hat{c}^\dagger_{k_1,\uparrow}\hat{c}_{k_2,\uparrow}\hat{c}^\dagger_{k_3,\downarrow}\hat{c}_{k_4,\downarrow}e^{i(k_1+k_3-k_2-k_4)l} = \\ &= \frac{U}{N}\sum_{k_1,k_2,k_3,k_4}\hat{c}^\dagger_{k_1,\uparrow}\hat{c}_{k_2,\uparrow}\hat{c}^\dagger_{k_3,\downarrow}\hat{c}_{k_4,\downarrow}\delta(k_1+k_3-k_2-k_4) = \frac{U}{N}\sum_{klq}\hat{c}^\dagger_{k,\uparrow}\hat{c}_{k-q,\uparrow}\hat{c}^\dagger_{l,\downarrow}\hat{c}_{l+q,\downarrow} \end{aligned} \tag{2.3}$$

What we see here is that the first term is diagonal in the reciprocal basis. We will treat the second term as a perturbation to the tight binding Hamiltonian, $H_L = \frac{p^2}{2m} + V_L\sin^2(x)$

(L stands for "lattice") and it can be diagonalized using Bloch functions. However, instead of 2.3, the interaction potential will generalized, moving from the simple contact model to a more general one with a finite height and width. In this way we will use the second quantized form of a first quantized potential:

$$V_{int} = \frac{1}{2}\sum_{k\neq l} V_{int}(x_k, x_l), \tag{2.4}$$

where $V_{int}(x_k, x_l) = V_{int}(|x_k - x_l|)$, and we will take it to be a soft sphere potential and a Calogero-Sutherland potential (see, [7] and [8]). The second quantized form of 2.4 is:

$$V_{int} = \frac{1}{2}\sum_{klmn} \hat{c}_k^\dagger \hat{c}_l^\dagger \langle kl| V_{int} |mn\rangle \hat{c}_n \hat{c}_m \tag{2.5}$$

Once H_L has been diagonalized, we will be able to write a diagrammatic expansion using the single particle Green's function and the matrix elements in 2.5. Then, we will compute the quasi particle parameters as a function of V_{int}.

The original Hubbard model was proposed in 1963 to describe electrons in a solid. However, recently it has been extensively studied for the cold atom optical trapping, in its version for bosons: the Bose-Hubbard model ([18]).

A brief review of some useful aspects of solid state physics

To solve the problem of many interacting electrons in an optical lattice we have to solve first the problem of a single electron in this lattice. The potential $V(x) = V_0 \sin^2(k_L x)$ of the optical lattice is a periodic potential, therefore the single particle eigenbasis can be chosen to be Bloch's functions. These functions are the basis we will use to compute the interaction potential matrix elements, and will set the framework to work with diagrammatic expansions theory.

In this chapter we state Bloch's theorem and highlight the details we will need for our further study.

3.1 Bloch's theorem

In this section we review the basic physics of a single particle subject to a $1D$ periodic potential, in our case $V(x) = V_0 \sin^2(k_L x) \rightarrow V(x+d) = V(x)$ for $d = \dfrac{\pi}{k_L}$. The Schrodinger equation for a particle of mass m is:

$$\left(\frac{\hat{p}^2}{2m} + V(x) \right) \psi = \epsilon \psi \tag{3.1}$$

Bloch's theorem states that the eigenstates of this Hamiltonian can be chosen to have the form:

$$\psi_q^n(x) = e^{iqx} u_q^n(x) \tag{3.2}$$

Where $u_q^n(x) = u_q^n(x+d)$, and q is a quantum number called crystal wave number which we will show it must be real. Also, n is a discrete index, called the band index. Notice that equation 3.2 is equivalent to:

$$\psi_q^n(x + rd) = e^{iqrd} \psi_q^n(x) \tag{3.3}$$

For any integer r. From equation 3.3, one can get 3.2 defining $u(x) = e^{-iqx}\psi(x)$ such that $u(x+d) = u(x)$).

Now, we proof Bloch's theorem ([5]). First, define for all integer n, $T_n = e^{-ind\hat{p}/\hbar}$, a translation operator, that satisfies $T_n\psi(x) = \psi(x + nd)$. Now, since the potential is periodic, we can show that $\hat{H}$ commutes with all the T_n, taking into account that T_n commutes with $\frac{\hat{p}^2}{2m}$:

$$T_n\hat{H}T_n^{-1} = T_n\frac{\hat{p}^2}{2m}T_n^{-1} + T_nV(x)T_n^{-1} = \frac{\hat{p}^2}{2m} + V(x + nd) = \hat{H} \tag{3.4}$$

Also, the composition of two translation is another translation, and it does not depend on the order of the composition:

$$T_nT_{n'} = T_{n'}T_n = T_{n+n'} \tag{3.5}$$

Therefore, the set of all T_n together with H form a set of commuting operators. Hence, the eigenstate of H can be chosen to be simultaneous eigenstates of all the T_n:

$$\begin{aligned} \hat{H}\,|\psi\rangle &= \epsilon\,|\psi\rangle \\ T_n\,|\psi\rangle &= f(n)\,|\psi\rangle \end{aligned} \tag{3.6}$$

Where $f(n)$ is the eigenvalue of ψ when acted by T_n. Equation 3.5 implies that $f(n + n') = f(n)f(n')$, and if we write $f(1) = e^{iqd}$ (generally q can be a complex number, but we will show that boundary conditions imply it must be real) we would have $f(n) = e^{iqnd}$, that is:

$$\psi(x + nd) = T_n\psi(x) = e^{iqnd}\psi(x) \tag{3.7}$$

Which is the same as 3.3 (notice that now we can define $u(x) = e^{-iqx}\psi(x)$ satisfying $u(x+d) = u(x)$). This completes the proof.

3.2 Boundary conditions

Let's now examine in more detail the quantum number q introduced in the Bloch's theorem. So far we have seen that this number can be any complex number, but the boundary conditions of the system will restrict it to a few real numbers. We impose periodic boundary conditions, which means that if our system has length L, then $\psi(x + L) = \psi(x)$ (i.e. we are identifying the beginning and ending points of the lattice). In the case of the optical lattice, $L = Nd$, where N is the number of sites in the lattice, or minima of the potential, and d is the length of each cell in the lattice, that is, the periodicity of the potential ($d = \frac{\pi}{k_L}$). Now, if we impose this boundary condition to a Bloch's function $\psi_q^n(x)$ we obtain:

$$e^{iqL} = 1 \to qL = 2\pi s, \quad s \in \mathbb{Z} \tag{3.8}$$

Therefore $q = \frac{2k_L s}{N}$. Now, we don't have to consider all integers s, because by changing $q \to q + 2k_L$, one gets redundant information (since $e^{i(q+2k_L)x} = e^{iqx}e^{i2k_L x}$ and $e^{i2k_L x}$ is periodic with period d, and therefore can be merged into the $u_q^n(x)$ function). So we need to consider only N different values of s, and we chose $s = -\frac{N}{2}, \ldots, \frac{N-1}{2}$ (assuming N is even). With this selection, the corresponding q's are said to be in the first Brilluin zone.

In three dimensions q is a vector, and it can be seen as a vector in the reciprocal lattice.

3.3 Band theory

For a fixed q there can be several eigenfunctions of the form 3.2, which we will suppose to form a discrete set. These are indexed with the number n, and have energy E_q^n. If we see E_q^n as a function of q and n, then, for a fixed n it will map a region of allowed energies (we are considering q to vary continuously, but in our case it is discrete). This region of energies is known as an energy band. The study of energy bands, known as electronic structure, is capital in the analysis of conductivity effects in material science. Following the procedure explained in Chapter 3, we plot E_q^n as a function of q for several values of n, and for a low and a high value of V_0, in figure 3.1. In the limit $V_0 \to 0$ the energies E_q^n are those of a free particle, and when plotted as in figure 3.1, it shows a parabolic shape in which the $n = 1$ level is connected to the $n = 2$ at the highest and lowest value of q (i.e., $q = \pm k_L$). As we increase V_0 each n level becomes narrower, and the gap between bands is larger. Remember that in our problem we suppose that all the electrons are in the first band, now we are able to see when this hypothesis would be valid. The thermal fluctuations of the system must be smaller than the gap between the first and the second band, that is $k_B T << \Delta E_{1\to 2}$, and this is true for low temperatures and for high potential depth.

In this project we work only with the first band eigenfunctions. The basis of the Hilbert space will be approximated by the $\psi_q^n(x)$ with $n = 1$ functions, which do not form a complete set. This is a common approximation in tight binding models, and it is at the core of the Hubbard model. This is a good approximation only at sufficiently low temperatures, so that all the particles are in the lowest Bloch's band.

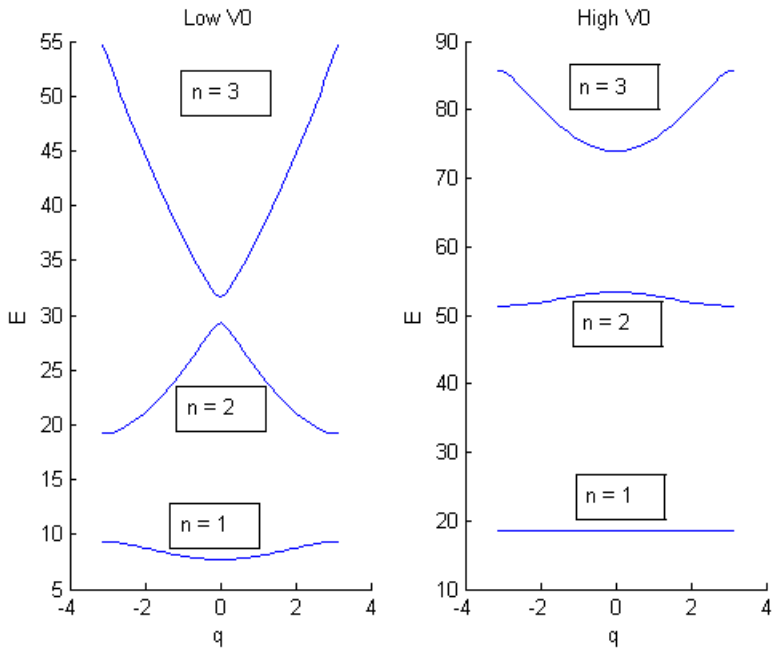

Figure 3.1: Band energies in the potential $V(x) = V_0 \sin^2(k_L x)$

Feynman Diagrams

In this chapter we will explain the required theoretical background for this project. However, the rigorous derivation of the rules for computing Feynman diagrams is extremely complicated and long, therefore we will only present this rules and use them for some example (for a more detailed deviation see [1], [2] and [3]). First we need to introduce the single particle Green's function, also known as propagator, which is a powerful concept to study any kind of many particle system, and which we will calculate with the aid of Feynman diagrams.

The general idea of this project is as follows. First we will solve numerically the non-interacting case, that is, the problem of a single particle in an optical lattice potential. Once this is done we will have the free Green's function, or free propagator $G_0(k_2, k_1, t_2 - t_1)$. Then we will activate the interaction between particles, and we will calculate the interacting Green's function $G(k_2, k_1, t_2 - t_1)$ in terms of $G_0(k_2, k_1, t_2 - t_1)$ and the interaction potential matrix elements using Feynman diagrams.

4.1 Single particle Green's funcion

First, let's introduce the time-ordering operator, T, which is defined by

$$T[A(t_1)B(t_2)] = \begin{cases} A(t_1)B(t_2), & \text{for} \quad t_1 > t_2 \\ -B(t_2)A(t_1), & \text{for} \quad t_1 < t_2 \end{cases} \tag{4.1}$$

In the case T acts on more than two operators, the result is the rearrangement of the operators so that time decreases from left to right, times $(-1)^P$ where P is the number of transpositions of operators required to get the operators in the proper time order. For example, if $t_1 < t_2 < t_3 < t_4$:

$$T[A(t_3)B(t_4)C(t_2)D(t_1)] = (-1)^5 D(t_1)C(t_2)A(t_3)B(t_4) \tag{4.2}$$

Now, let $|\Phi_0\rangle$ be the normalized ground state in the Heisenberg picture of the interacting system, and let $\psi(x,t)$, $\psi^\dagger(x,t)$, be the Heisenberg operators that annihilate/create a particle at the space-spin point x at time t, respectively. Then, the spatial single particle Green's function is defined by:

$$iG(x_2, x_1, t_2 - t_1) = \langle \Phi_0 | \, T[\psi(x_2, t_2)\psi^\dagger(x_1, t_1)] \, | \Phi_0 \rangle \tag{4.3}$$

We can define the Green's function in any other basis as follows. Let $c_k(t)$, $c_k^\dagger(t)$ the anihilation/creation operators of a particle in state k at time t. Then:

$$iG(k_2, k_1, t_2 - t_1) = \langle \Phi_0 | \, T[c_{k_2}(t_2) c^\dagger_{k_1}(t_1)] \, | \Phi_0 \rangle \tag{4.4}$$

Note that $c_k(t)$, $c^\dagger_k(t)$ are the annihilation and creation operatros in the Heisenberg picture:

$$\begin{aligned} c^\dagger_k(t) &= e^{iHt} c^\dagger_k e^{-iHt} \\ c_k(t) &= e^{iHt} c_k e^{-iHt} \end{aligned} \tag{4.5}$$

Where c_k and $c^\dagger_k$ are the ordinary creation/anihilation operators introduced in Chapter 1.

We will mostly use the second definition the the Green's function. We will first solve the non-interacting problem for the optical lattice potential, and we will get a basis of eigenfunctions that will be the ones we use to write the Green's function.

Now we will show what is the meaning of the Green's function, for that we insert 4.5 in 4.4, and let $|\Phi_0(t)_S\rangle$ be the ground state in the Schrodinger picture at time t, $|\Phi_0(t)_S\rangle = e^{-iE_0 t} |\Phi_0\rangle$.

$$\begin{aligned} iG(k_2, k_1, t_2 - t_1) &= \langle \Phi_0 | \, T[c_{k_2}(t_2) c^\dagger_{k_1}(t_1)] \, | \Phi_0 \rangle = \\ &= \langle \Phi_0 | \, e^{iHt_2} c_{k_2} e^{-iHt_2} e^{iHt_1} c^\dagger_{k_1} e^{-iHt_1} \, | \Phi_0 \rangle \, \theta(t_2 - t_1) \\ &+ \langle \Phi_0 | \, e^{iHt_1} c^\dagger_{k_1} e^{-iHt_1} e^{iHt_2} c_{k_2} e^{-iHt_2} \, | \Phi_0 \rangle \, \theta(t_1 - t_2) \\ &= \langle \Phi_0(t_2)_S | \, c_{k_2} e^{-iH(t_2 - t_1)} c^\dagger_{k_1} \, | \Phi_0(t_1)_S \rangle \, \theta(t_2 - t_1) \\ &+ \langle \Phi_0(t_1)_S | \, c^\dagger_{k_1} e^{-iH(t_1 - t_2)} c_{k_2} \, | \Phi_0(t_2)_S \rangle \, \theta(t_1 - t_2) \end{aligned} \tag{4.6}$$

Now we can clearly see what the Green's function is. For $t_2 > t_1$ it is the component of $e^{-iH(t_2 - t_1)} c^\dagger_{k_1} |\Phi_0(t_1)_S\rangle$ along $c^\dagger_{k_2} |\Phi_0(t_2)_S\rangle$, that is, the probability amplitude that the state at t_2 when a particle in state k_1 was added at t_1 is in the state with one particle in state k_2 added at time t_2. Likewise, for $t_1 > t_2$ the Green's function is the probability amplitude that adding a hole at time t_2 in state k_2 we find it in state k_1 at time t_1.

Suppose we have already diagonalized the non-interacting Hamiltonian, $H_0 = \sum_k \epsilon_k c^\dagger_k c_k$ and suppose that the ground state of the non-interacting system is the state with all the states with energies $k < k_F$ occupied so that the ground state energy is $E_0 = \sum_{k<k_F} \epsilon_k$. Then, the Green's function of this system, which is called free Green's function or free propagator can be obtained from 4.6, taking $t_2 - t_1 = t$, $iG_0(k_2, k_1, t) = iG_0(k_2, k_1, t - 0)$:

$$\begin{aligned} iG_0(k_2, k_1, t) &= \langle \Phi_0 | \, e^{iH_0 t} c_{k_2} e^{-iH_0 t} c^\dagger_{k_1} \, | \Phi_0 \rangle \, \theta(t) \\ &- \langle \Phi_0 | \, c^\dagger_{k_1} e^{iH_0 t} c_{k_2} e^{-iH_0 t} \, | \Phi_0 \rangle \, \theta(-t) \\ &= e^{iE_0 t} \langle \Phi_0 | \, c_{k_2} e^{-iH_0 t} c^\dagger_{k_1} \, | \Phi_0 \rangle \, \theta(t) \\ &- e^{-iE_0 t} \langle \Phi_0 | \, c^\dagger_{k_1} e^{iH_0 t} c_{k_2} \, | \Phi_0 \rangle \, \theta(-t) \end{aligned} \tag{4.7}$$

Now, if $k_1 > k_F$, then $c^\dagger_{k_1} |\Phi_0\rangle$ is an eigenstate of the Hamiltonian with energy $E_0 + \epsilon_{k_1}$. If $k_1 < k_F$ then $c^\dagger_{k_1} |\Phi_0\rangle = 0$. In the same way, if $k_2 < k_F$, then $c_{k_2} |\Phi_0\rangle$ is an eigenstate of the Hamiltonian with energy $E_0 - \epsilon_{k_2}$, otherwise it vanishes. Therefore:

$$\begin{aligned} iG_0(k_2, k_1, t) &= e^{iE_0 t} \langle\Phi_0| c_{k_2} e^{-i(E_0+\epsilon_{k_1})t} c^\dagger_{k_1} |\Phi_0\rangle \theta(t)\theta(k_1 - k_F) \\ &- e^{-iE_0 t} \langle\Phi_0| c^\dagger_{k_1} e^{i(E_0-\epsilon_{k_2})t} c_{k_2} |\Phi_0\rangle \theta(-t)\theta(k_F - k_2) \\ &= e^{-i\epsilon_{k_1} t} \langle\Phi_0| c_{k_2} c^\dagger_{k_1} |\Phi_0\rangle \theta(t)\theta(k_1 - k_F) \\ &- e^{-i\epsilon_{k_2} t} \langle\Phi_0| c^\dagger_{k_1} c_{k_2} |\Phi_0\rangle \theta(-t)\theta(k_F - k_2) \end{aligned} \tag{4.8}$$

Lastly, $\langle\Phi_0| c_{k_2} c^\dagger_{k_1} |\Phi_0\rangle = \delta_{k_1,k_2}$, so we usually write:

$$iG_0(k, t) = e^{-i\epsilon_k t} \{\theta(t)\theta(k - k_F) - \theta(-t)\theta(k_F - k)\} \tag{4.9}$$

However, when we perform Feynman diagrams we will mostly use them in the frequency domain, so we need $iG_0(k, w)$. To obtain it we will use the identities:

$$\begin{aligned} \theta(t) &= -\lim_{\eta\to 0} \frac{1}{2\pi i} \int_{-\infty}^{\infty} dw \frac{e^{-iwt}}{w + i\eta} \\ \theta(-t) &= \lim_{\eta\to 0} + \frac{1}{2\pi i} \int_{-\infty}^{\infty} dw \frac{e^{-iwt}}{w - i\eta} \end{aligned} \tag{4.10}$$

This can be verified by performing the integrals in the complex w plane. For the first case, $\theta(t)$, if $t > 0$ then the contour must be closed in the lower plane so that the exponential vanishes for large w. In that case, the contour would include a pole in $w = -i\eta$, with residue (-1). If $t < 0$, there is no pole, so the integral vanishes. Inserting 4.10 in 4.9 we obtain:

$$\begin{aligned} iG_0(k, t) &= \frac{i}{2\pi} \lim_{\eta\to 0} \int_{-\infty}^{\infty} dw \left(\frac{e^{-i(\epsilon_k+w)t}}{w + i\eta} \theta(k - k_F) + \frac{e^{-i(\epsilon_k+w)t}}{w - i\eta} \theta(k_F - k) \right) \\ &= \frac{i}{2\pi} \lim_{\eta\to 0} \int_{\infty}^{\infty} dw \left(\frac{e^{-iwt}}{w - \epsilon_k + i\eta} \theta(k - k_F) + \frac{e^{-iwt}}{w - \epsilon_k - i\eta} \theta(k_F - k) \right) \end{aligned} \tag{4.11}$$

Therefore, since:

$$iG_0(k, t) = \frac{1}{2\pi} \int_{-\infty}^{\infty} dw iG_0(k, w) e^{-iwt} \tag{4.12}$$

We conclude:

$$iG_0(k,w) = \lim_{\eta\to 0} \frac{i}{w - \epsilon_k + i\eta_k} \tag{4.13}$$

Where $\eta_k = +\eta$ when $k > k_F$ and $\eta_k = -\eta$ when $k < k_F$. Generally we will not write the limit but assume that at the end of our calculations we must make $\eta \to 0$.

4.2 Feynman diagrams

Suppose that we have already diagonalized the non-interacting Hamiltonian $H = \frac{p^2}{2m} + U$, where U is an external potential, in this project $U = \sin^2(kx)$. Then we will already know $G_0(k,w)$ as in 4.13, we can obtain $G(k,w)$, the interacting propagator, as a perturbation series from $G_0(k,w)$ and the matrix elements:

$$V_{klmn} = \int dx \int dx' \psi_k^*(x)\psi_l^*(x')V(|x-x'|)\psi_m(x)\psi_n(x') \tag{4.14}$$

Where we will take three different forms of $V(|x-x'|)$:

1. A delta potential $V(x) = V_{int}\delta(x)$
2. A soft sphere potential:
$$V(x) = \begin{cases} V_{int}, \text{ for, } |x| < r_0 \\ 0, \text{ elsewhere} \end{cases}$$
3. A Colagero-Sutherland potential:
$$V(x) = V_{int}\frac{\pi^2/L^2}{\sin\left(\frac{\pi}{L}x\right)^2} \tag{4.15}$$

Now we start drawing. Diagrammatically we will write $iG_0(k,w)$ as:

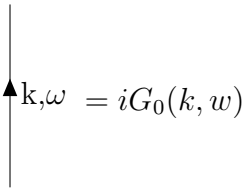

$$= iG_0(k,w) \tag{4.16}$$

Since we are drawing diagrams in the frequency domain, we have to label each line with the state of the particle k, and a frequency w. The interaction matrix element $-iV_{klmn}$ will be drawn with a wiggle line:

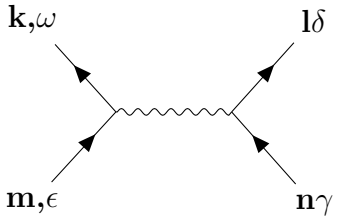

$$= -iV_{klmn} \tag{4.17}$$

This diagram is interpreted as follows: two particles in states m, n interact and exchange some momentum and scatter two new particles in states k, l. If the interaction is momentum conserving, which it will be in most cases, we can write $V_{klmn} = V_{(k-q)(l+q)kl}$, and now we can see that the particle in state k transfers a momentum q to the particle in state l. Now we will explain how to calculate $G(k, w)$ using Feynman diagrams. The rigorous derivation of the Feynman rules is too hard to be done in here, therefore we will only present the final result. This result states that the interacting propagator $iG(k, w)$ can be obtained as the sum of all topologically distinct connected diagrams which connect two endpoints labeled with k, w. To draw a nth order diagram we draw n wiggly lines and two external points and join all the $2n + 2$ vertex to each other with free propagator lines in such a way that each vertex has a leaving line and an entering line, except the two external vertex. If two diagrams can be deformed into each other we will only count one of them. Now each line we draw represents a factor $iG_0(k, w)$, so we shall label each line with momentum k and frequency w in such way that momentum and frequency is conserved in each interaction, that is, the sum of momenta before the interaction equals the sum of momenta after the interaction and the same for the frequencies. Then, we remove all diagrams which have a particle and a hole in the same state. Lastly, we can evaluate the diagrams with the following rules:

1. Each line gives a factor:

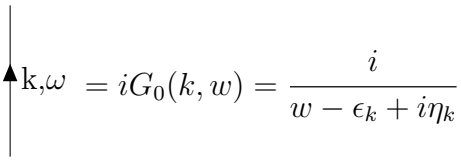

$$= iG_0(k, w) = \frac{i}{w - \epsilon_k + i\eta_k} \tag{4.18}$$

2. If a line closes in the same interaction line it gives a factor:

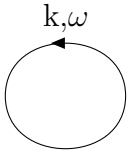

$$= iG_0(k, w)e^{iw0^+} \tag{4.19}$$

or

$$= iG_0(k, w)e^{iw0^+} \tag{4.20}$$

3. Each interaction line gives a factor:

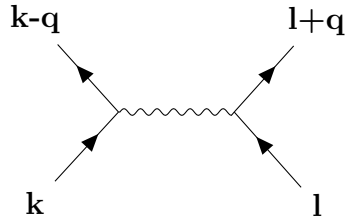

$$= -iV_{(k-q)(l+q)kl} = -iV_{klq} = -iV_q \tag{4.21}$$

These three notations for the potential are used, the third equality may hold if the interaction depends only in the transferred momentum. While deriving theoretical expressions we will use the first four-indexed notation, but at the end we will always write in the three-indexed notation. Notice that in the four-indexed notation the first index corresponds to the particle leaving the left vertex, the second corresponds to the particle leaving the right vertex and the third and fourth correspond to the particles entering the left and right vertex respectively. However, in the three-indexed notation, the first and second indexed correspond to the particles entering the left and right vertexes, while the third index corresponds to the transferred momentum.

4. For each loop that the propagator lines do we must add a factor of -1. For example, in the following diagram, known as single pair-bubble diagram we should multiply per -1:

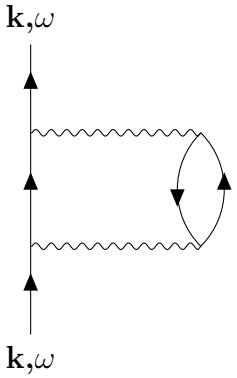

5. Finally, for any intermediate frequency w that appears in each propagator line we must perform an integral:

$$\int \frac{dw}{2\pi} \tag{4.22}$$

And, for any intermediate state p that appears in each propagator line we must sum over all p:

$$\sum_p \tag{4.23}$$

Since we have to integrate and sum over all intermediate frequencies and states, sometimes we don't label the propagator lines in the diagrams, because these labels are dummy labels.

As an example, we will evaluate the single pair-bubble diagram:

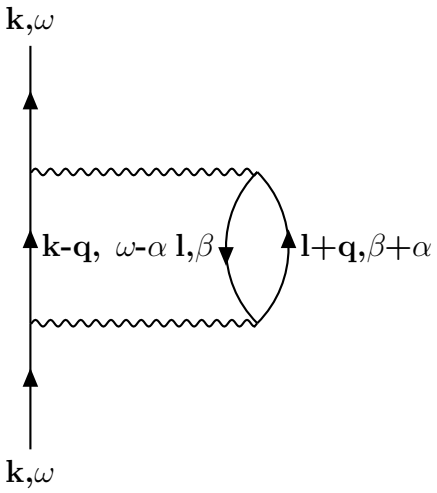

Following the stated rules we find that this diagram contributes with:

$$(-1)\int\frac{d\alpha}{2\pi}\int\frac{d\beta}{2\pi}\sum_q\sum_l(-iV_{kl(k-q)(l+q)})(-iV_{(k-q)(l+q)kl})\times \tag{4.24}$$
$$\times\left(iG_0(k,w)\right)^2\left(iG_0(k-q,w-\alpha)\right)(iG_0(l,\beta))(iG_0(l+q,\beta+\alpha))$$

An important result in Feynman diagrams theory is that we don't have to consider diagrams such that they can be divided into two separate diagrams by cutting only one point, for example:

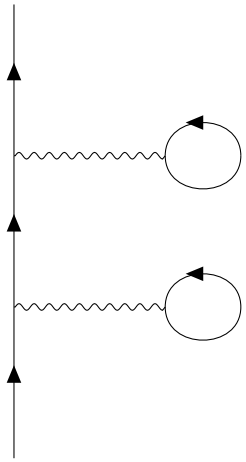

This kind of diagrams are called improper, and the diagrams that cannot be separated into two diagrams by cutting one point are called proper. We will show that we can easily sum over all diagrams that are composed by a fixed family of proper diagrams. The idea is that the contribution of each improper diagram factorized in the product of the proper diagrams, we can write it in diagrammatic way:

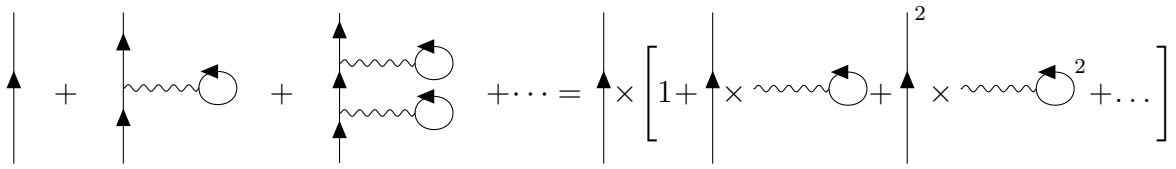

(4.25)

This can be summed as a geometric progression leading to:

$$iG(k,w) = \frac{1}{^{-1}\;\; - \;\;}$$

(4.26)

If instead we sum over all families of proper diagrams we obtain:

$$iG(k,w) = \frac{1}{^{-1}\;\; - \;\; \Sigma}$$

(4.27)

Where Σ is the sum of all proper diagrams, and it is called the self energy:

$$-i\Sigma(k,w) =$$

(4.28)

Now the different diagrams used to approximate $\Sigma(k,w)$ lead to different well-known approximations. The most important ones are the following:

1. The Hartree-Fock approximation uses the bubbles and open oysters diagrams, which are:

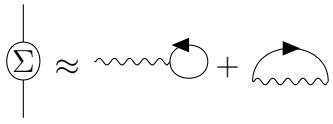

(4.29)

2. The random phase approximation (RPA) uses an infinite family of proper diagrams to approximate the self energy. These diagrams are the ring diagrams:

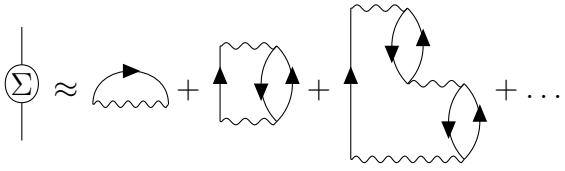

(4.30)

3. The ladder approximation uses the ladder diagrams to approximate the self energy, which are the diagrams with only one hole line:

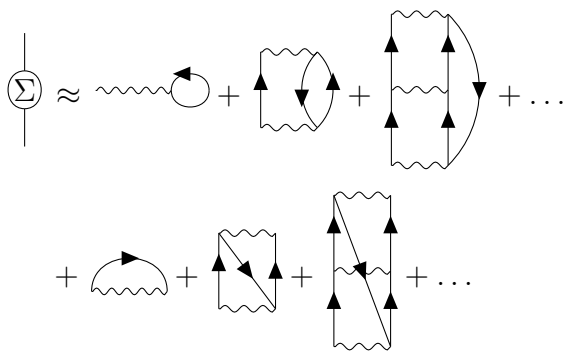

(4.31)

Now we will obtain the expressions for $\Sigma(k, w)$ for this three approximations using the rules for evaluating Feynman diagrams. Later we will use this expressions to obtain the energy correction of the electrons.

4.2.1 Hartree-Fock

Following the Feynman rules we can translate the diagrams in 4.29:

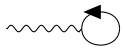

$$\begin{aligned} l,\epsilon \; &= (-1)\sum_l \int \frac{d\epsilon}{2\pi}(-iV_{klkl})iG_0(l,\epsilon)e^{i\epsilon 0^+} \\ &= (-1)\sum_l \int \frac{d\epsilon}{2\pi}(-iV_{klkl})\frac{i}{\epsilon-\epsilon_l+i\eta_l}e^{i\epsilon 0^+} \\ &= (-1)\sum_l i(-iV_{klkl})i\theta(\epsilon_F-\epsilon_l) \\ &= -i\sum_{\epsilon_l<\epsilon_F} V_{klkl} \end{aligned} \tag{4.32}$$

Where the integral over ϵ has been performed by closing the integration path with a semicircle in the upper half-plane to unsure the convergence of the factor $e^{i\epsilon 0^+}$. Analogously we can evaluate the second diagram in the Hartree-Fock approximation:

$$\begin{aligned} &= \sum_l \int \frac{d\epsilon}{2\pi}(-iV_{lkkl})iG_0(l,\epsilon)e^{i\epsilon 0^+} \\ &= \sum_l i(-iV_{lkkl})i\theta(\epsilon_F-\epsilon_l) \\ &= i\sum_{\epsilon_l<\epsilon_F} V_{lkkl} \end{aligned} \tag{4.33}$$

Therefore the self-energy in the Hartree-Fock approximation is, 4.28:

$$\Sigma(k,\omega) = \sum_{\epsilon_l<\epsilon_F} V_{klkl} - V_{lkkl} \tag{4.34}$$

We can write this expression using three indexes for the potential matrix elements, which will be more useful for computational proposes:

$$\Sigma(k,\omega) = \sum_{\epsilon_l<\epsilon_F} V_{kl0} - V_{kl(k-l)} \tag{4.35}$$

There is something we have not been taking into account: spin. In formula 4.34 we should multiply times 2, because for each state k below the Fermi surface there are two particles in that state, one with spin up, and another with spin down. However, in the Hubbard model only interaction between particles with different spin are allowed. Since we are developing from Hubbard model, we will take this kind of interaction. Therefore, one particle can only interact with particles with opposite spin, and that is the reason we can only sum once in 4.34.

4.2.2 RPA approximation

Now we will obtain the self-energy for the family of ring diagrams. For this calculation we will approximate $V_{kpq} = V_q$, which in the cases we will study is not a bad approximation. Now we only have to manipulate 4.30:

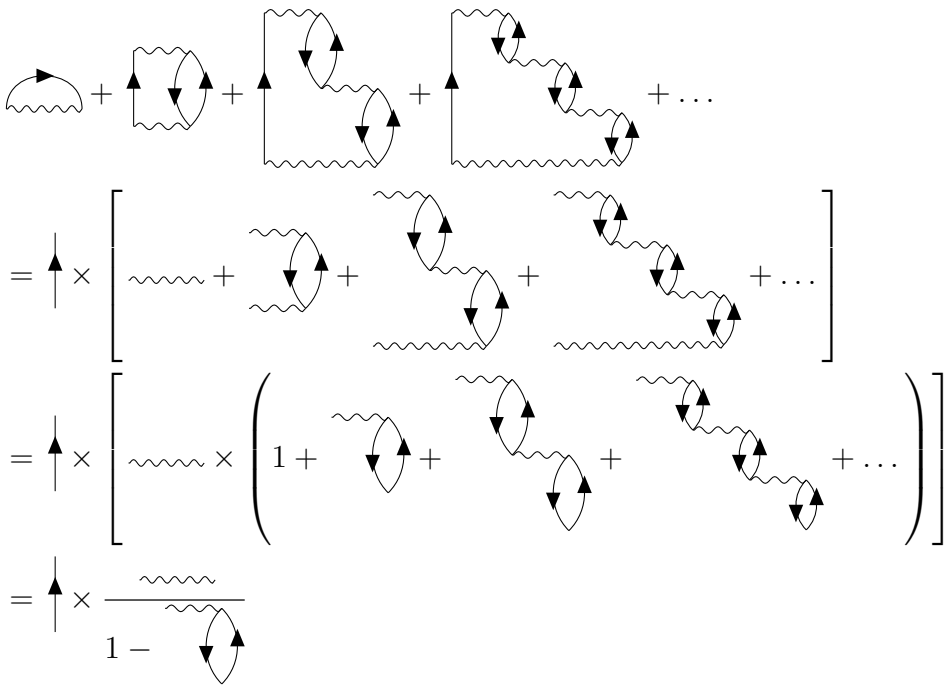

(4.36)

Now we have to translate this diagrammatic equation. First, let q be the momentum transferred between rings (at the end we will sum over q):

$$\begin{aligned}
&= (-1)\sum_p \int \frac{d\beta}{2\pi} iG_0(p+q,\beta+\epsilon) iG_0(p,\beta)(-iV_q) \\
&= (-1)\sum_p \int \frac{d\beta}{2\pi}(-iV_q)\frac{i}{\beta+\epsilon-\epsilon_{p+q}+i\eta}\frac{i}{\beta-\epsilon_p-i\eta} \\
&= (-1)\sum_p i(-iV_q)\frac{i}{\epsilon+\epsilon_p-\epsilon_{p+q}+i\eta} i \\
&= +\sum_p \frac{V_q}{\epsilon+\epsilon_p-\epsilon_{p+q}+i\eta}
\end{aligned} \tag{4.37}$$

The integral in the second step is performed by closing the integration path along the upper half complex β-plane. There is only one pole in $\beta = \epsilon_p + i\eta$ with residue $(-iV_q)\dfrac{i}{\epsilon+\epsilon_p-\epsilon_{p+q}+i\eta} i$.

Now, using 4.36, summing over the transferred momentum and integrating the transferred frequency, the self energy in the RPA approximation is:

$$\begin{aligned}
\Sigma(k,\omega) &= \sum_q \int \frac{d\epsilon}{2\pi} iG_0(k-q,\omega-\epsilon)\frac{-iV_q}{1-\sum_p \dfrac{V_q}{\epsilon+\epsilon_p-\epsilon_{p+q}+i\eta}} \\
&= \sum_q \int \frac{d\epsilon}{2\pi}\frac{i}{\omega-\epsilon-\epsilon_{k-q}+i\eta}\frac{V_q}{1-\sum_p \dfrac{-iV_q}{\epsilon+\epsilon_p-\epsilon_{p+q}+i\eta}} \\
&= \sum_q i(-i)\frac{-iV_q}{1-\sum_p \dfrac{V_q}{\omega-\epsilon_{k-q}+\epsilon_p-\epsilon_{p+q}+i\eta}} \\
&= (-i)\sum_q \frac{V_q}{1-\sum_p \dfrac{V_q}{\omega-\epsilon_{k-q}+\epsilon_p-\epsilon_{p+q}+i\eta}}
\end{aligned} \tag{4.38}$$

4.2.3 Ladder approximation

In this approximation, as well as in the RPA we have to sum over an infinite family of diagrams. To do so we will first define:

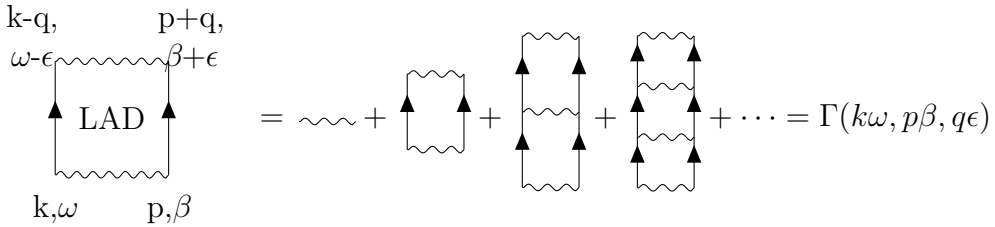

$$= \sim\!\sim + \square + \square\!\square + \square\!\square\!\square + \cdots = \Gamma(k\omega, p\beta, q\epsilon) \tag{4.39}$$

Where the incoming and outgoing particles are the same for all the diagrams in the sum and are those of the diagram in the left hand side. Now we can obtain an integral equation for $\Gamma(k\omega, p\beta, q\epsilon)$:

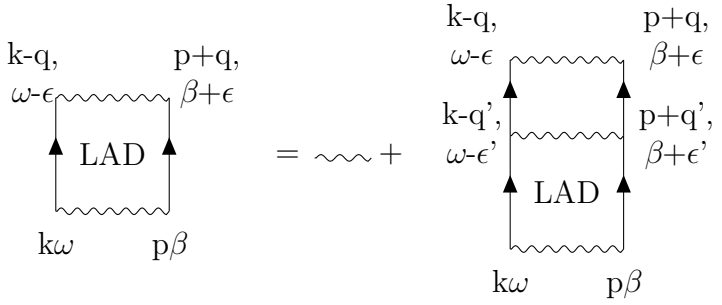

(4.40)

We can translate this to:

$$\begin{aligned}\Gamma(k\omega, p\beta, q\epsilon) = -iV_{kpq} + \sum_{q'} \int \frac{d\epsilon'}{2\pi} \Gamma(k\omega, p\beta, q'\epsilon') \times \\ \times\, iG_0(k-q', \omega-\epsilon') iG_0(p+q', \beta+\epsilon')(-iV_{(k-q')(p+q')(q-q')})\end{aligned} \tag{4.41}$$

We will now obtain $\Gamma(p_1\epsilon_1, p_2\epsilon_2, q\omega)$, first we integrate

$$\begin{aligned}\Gamma(k\omega, p\beta, q\epsilon) &= -iV_{kpq} + \sum_{q'} \int \frac{d\epsilon'}{2\pi} \Gamma(k\omega, p\beta, q'\epsilon') \frac{i}{\omega - \epsilon' - \epsilon_{k-q'} + i\eta} \frac{V_{(k-q')(p+q')(q-q')}}{\beta + \epsilon' - \epsilon_{p+q'} + i\eta} \\ &= -iV_{kpq} + \sum_{q'} i\Gamma(k\omega, p\beta, q'(\beta - \epsilon_{p+q'} + i\eta))(-i) \frac{V_{(k-q')(p+q')(q-q')}}{\omega + \beta - \epsilon_{p+q'} - \epsilon_{k-q'} + i\eta} \\ &= -iV_{kpq} + \sum_{q'} \frac{\Gamma(k\omega, p\beta, q'(\omega - \epsilon_{p+q'} + i\eta)) V_{(k-q')(p+q')(q-q')}}{\omega + \beta - \epsilon_{p+q'} - \epsilon_{k-q'} + i\eta}\end{aligned} \tag{4.42}$$

Therefore:

$$\Gamma(k\omega, p\beta, q\epsilon) = \frac{-iV_{kpq}}{1 - \sum_{q'} \frac{V_{(k-q')(p+q')(q-q')}}{\omega + \beta - \epsilon_{k-q'} - \epsilon_{p+q'} + i\eta}} \tag{4.43}$$

Now we can write the full self-energy of the ladder approximation, 4.31, in terms of $\Gamma(k\omega, p\beta, q\epsilon)$ as:

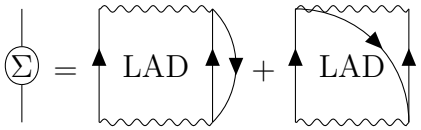

(4.44)

Where:

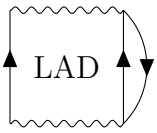

$$\begin{aligned} &= (-1)\sum_p \int \frac{d\beta}{2\pi}\Gamma(k\omega, p\beta, 00) i G_0(p,\beta) \\ &= (-1)\sum_p i\Gamma(k\omega, p(\epsilon_p + i\eta), 00) i \\ &= \sum_p \frac{-iV_{kp0}}{1 - \sum_{q'} \dfrac{V_{(k-q')(p+q')(-q')}}{\omega + \epsilon_p - \epsilon_{k-q'} - \epsilon_{p+q'} + i\eta}} \end{aligned} \tag{4.45}$$

And:

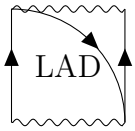

$$\begin{aligned} &= \sum_p \int \frac{d\beta}{2\pi}\Gamma(k\omega, p\beta, (k-p)(\omega-\beta)) i G_0(p,\beta) \\ &= \sum_p i\Gamma(k\omega, p(\epsilon_p + i\eta), (k-p)(\omega-\epsilon_p)) i \\ &= \sum_p \frac{iV_{kp(k-p)}}{1 - \sum_{q'} \dfrac{V_{(k-q')(p+q')(k-p-q')}}{\omega + \epsilon_p - \epsilon_{k-q'} - \epsilon_{p+q'} + i\eta}} \end{aligned} \tag{4.46}$$

We conclude:

$$\Sigma(k,\omega) = \sum_p \frac{V_{kp0} - V_{kp(k-p)}}{1 - \sum_{q'} \dfrac{V_{(k-q')(p+q')(k-p-q')}}{\omega + \epsilon_p - \epsilon_{k-q'} - \epsilon_{p+q'} + i\eta}} \tag{4.47}$$

4.3 Quasi particles

So far we have deduced different approximations to the self-energy, which is related to the Green's function with 4.27, a diagrammatic equation which can be translated as:

$$iG(k,w) = \frac{i}{w - \epsilon_k - \Sigma(k,w) + i\delta_k} \tag{4.48}$$

Now, the complex poles of $iG(k,w)$ gives the energy and lifetime of the electron. This can be easily shown, free Green's function in time is, according to 4.9, $iG_0(k,t) = e^{-i\epsilon_k t}$ if $k > k_F$ and $t > 0$. A quasi particle is like a free particle but with energy ϵ'_k and lifetime τ_k, so in the Green's function we have to change ϵ_k for ϵ'_k and multiply by and exponential decay of τ_k: $iG(k,t) = e^{-i\epsilon'_k t}e^{-t/\tau_k}$, whose Fourier transform is $iG(k,w) = \dfrac{1}{w - \epsilon'_k - i\tau_k}$. Therefore we have to find the poles of 4.48:

$$w - \epsilon_k - \Sigma(k,w) + i\delta_k = 0 \tag{4.49}$$

If $\Sigma(k,w)$ is small, the first order solution of this equation is obtained from the zeroth order solution $w = \epsilon_k$ as:

$$w = \epsilon_k + \Sigma(k,\epsilon_k) \tag{4.50}$$

The real and imaginary part of this pole are the energy and lifetime of the electron, respectively. Therefore, we conclude that the energy correction to the quasi particles is:

$$\Delta\epsilon_k = Re\{\Sigma(k,\epsilon_k)\} \tag{4.51}$$

In the next chapter, we will obtain $\Sigma(k,w)$ numerically, but we will only present $\Delta\epsilon_k$ as a function of the interaction potential parameter.

Numerical results

5.1 Diagonalizing the 1D non-interacting problem

Here we will diagonalize the Hamiltonian of a single electron in an optical lattice potential of the form:

$$V(x) = V_L \sin^2(k_L x) \tag{5.1}$$

This is a periodic potential since $V(x+d) = V(x)$ for $d = \dfrac{\pi}{k_L}$, with d the lattice constant. If N is the number of cells in the optical lattice and d is the lattice parameter, $L = Nd$ is the length of the system. The single particle Hamiltonian is:

$$\hat{H} = \frac{\hat{p}^2}{2m} + V(x) \tag{5.2}$$

According to Bloch's theorem, the eigenfunctions of this Hamiltonian can have the form:

$$\psi_q^n(x) = e^{iqx} u_q^n(x) \tag{5.3}$$

Where $u(x+d) = u(x)$ and $q = \dfrac{2\pi n}{Nd} = \dfrac{2nk_L}{N}$, we can choose $n = -N/2, \ldots, (N-1)/2$ so that q is in the first Brilluin zone. Notice that we will only work with $n = 1$, the first electronic band, and we will use $\psi_q^1(x)$ as a basis of the Hilbert space, even though it is not complete. This is an approximation done in the Hubbard model.

The eigenvalue problem we have to solve is:

$$\frac{\hat{p}^2}{2m}\psi_q^n(x) + V(x)\psi_q^n(x) = E_q^n \psi_q^n(x) \tag{5.4}$$

Inserting 5.3 in 5.4 we get:

$$\frac{(\hat{p} - q\hbar)^2}{2m} u_q^n(x) + V(x) u_q^n(x) = E_q^n u_q^n(x) \tag{5.5}$$

We can now Fourier transform $u_q^n(x)$ and $V(x)$:

$$u_q^n(x) = \sum_l c_q^{n,l} e^{2ilk_L x} \tag{5.6}$$

$$V(x) = \frac{V_L}{4}(2 - e^{2ik_L x} - e^{-2ik_L x}) \tag{5.7}$$

Inserting 5.6 and 5.7 in 5.5 we get:

$$\sum_l \left\{ \left(\frac{\hbar^2}{2m}(q - 2lk_L)^2 + \frac{V_L}{2} \right) c_q^{n,l} - \frac{V_L}{4} c_q^{n,l+1} - \frac{V_L}{4} c_q^{n,l-1} \right\} = E_q^n c_q^{n,l} \tag{5.8}$$

That is:

$$\sum_{l'} H_{l,l'} c_q^{n,l'} = E_q^n c_q^{n,l} \tag{5.9}$$

With

$$\begin{aligned} H_{l,l} &= \frac{\hbar^2}{2m}(q - 2lk_L)^2 + \frac{V_L}{2} \\ H_{l,\pm 1} &= -\frac{V_L}{4} \\ H_{l,l'} &= 0 \quad if \quad |l - l'| > 1 \end{aligned} \tag{5.10}$$

This is a tridiagonal system that can be solved numerically by truncating the maximum value of l. To know where to truncate we did a calculation using $l = -L_{max}, \ldots, L_{max}$ first with $L_{max} = 5$ and then with $L_{max} = 10$. The results were identical, that is, the coefficients $c_q^{n,l}$ didn't change at all, nor the energies. Moreover, we verified that $c_q^{n,l}$ rapidly vanishes for $|l| > 5$. In later calculations we will allways use $L_{max} = 10$.

Next, in figure 5.1 we plot $\psi_q^1(x)$ for $N = 10$. This is a plot in the complex plane, this way we can clearly see the Bloch's form of the function: each time we move to a different site in the lattice, i.e. each time we change $x \to x + d$ the wave functions is rotated a fixed angle in the complex plane, that is, it is multiplied by a factor of e^{iqd}. For this reason the graphic looks like a flower, each site in the optical lattice is a petal in the flower, and the number of petals in the flower is the number of sites in the lattices, $N = 10$.

5.2 Free Green's function

Now that we have already found a basis of eigenfunction for the non interacting Hamiltonian, we can write down the Free Green's function for this system. According to 4.9:

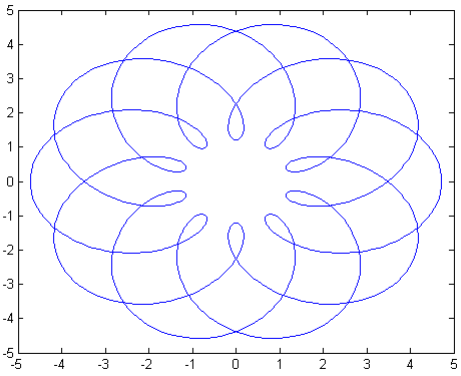

Figure 5.1: $\psi_q^1(x)$ for $N = 10$, we can see the flower-like form of the Bloch's functions

$$iG_0(k,t) = e^{-i\epsilon_k t}\left\{\theta(t)\theta(k-k_F) - \theta(-t)\theta(k_F-k)\right\} \tag{5.11}$$

Remember that iG_0 is local in spin space, that is, $iG_0^{s,s'}(k,t) = \delta(s,s')iG_0(k,t)$.

To get the position dependant Green function we use $\hat{\psi}(xt) = \sum_q \psi_q(x)\hat{c}_q(t)$. Where $\hat{c}_q(t)$ is the creation operator of a particle with crystal momentum q and Bloch index $n = 1$.

$$\begin{aligned} iG_0(x,x',t) &= \langle\Phi_0|\, T[\hat{\psi}(xt)\hat{\psi}^\dagger(x'0)]\,|\Phi_0\rangle \\ &= \sum_q \psi_q(x)\psi_q^*(x')\,\langle\Phi_0|\, T[\hat{c}_q(t)\hat{c}_q^\dagger(0)]\,|\Phi_0\rangle \\ &= \sum_q \psi_q(x)\psi_q^*(x')iG_0(qt) \\ &= \sum_q e^{-i\epsilon_q t}\psi_q(x)\psi_q^*(x')\left\{\theta(t)\theta(k-k_F) - \theta(-t)\theta(k_F-k)\right\} \end{aligned} \tag{5.12}$$

Now, these $\psi_q(x)$ are the same as those in 5.3, which we have computed. Thus, we can obtain this Green function easily and next we plot some graphics of $G_0(x,x',t)$ for x being a potential minimum and for different times, as shown in 5.2

In these plots the horizontal axis represents the x axis, and each integer is a potential minimum. We plotted the norm squared of $G_0(x,x',t')$, which can be interpreted as the probability density that a particle at x in $t = 0$ will be found in x' at time t. We can see how the particle spread all over the lattice as time goes on. Also, we can compute the ground state energy from the free Green function. In each of the simulations we performed, we verified that this energy coincides with the sum of the energy of each particle.

5.3 Interacting Green's function and energy correction

In this section we will use the results of section 4.2 to compute the full interaction Green's function. Firstly, we need to compute the matrix elements V_{klmn}, which we will first compute

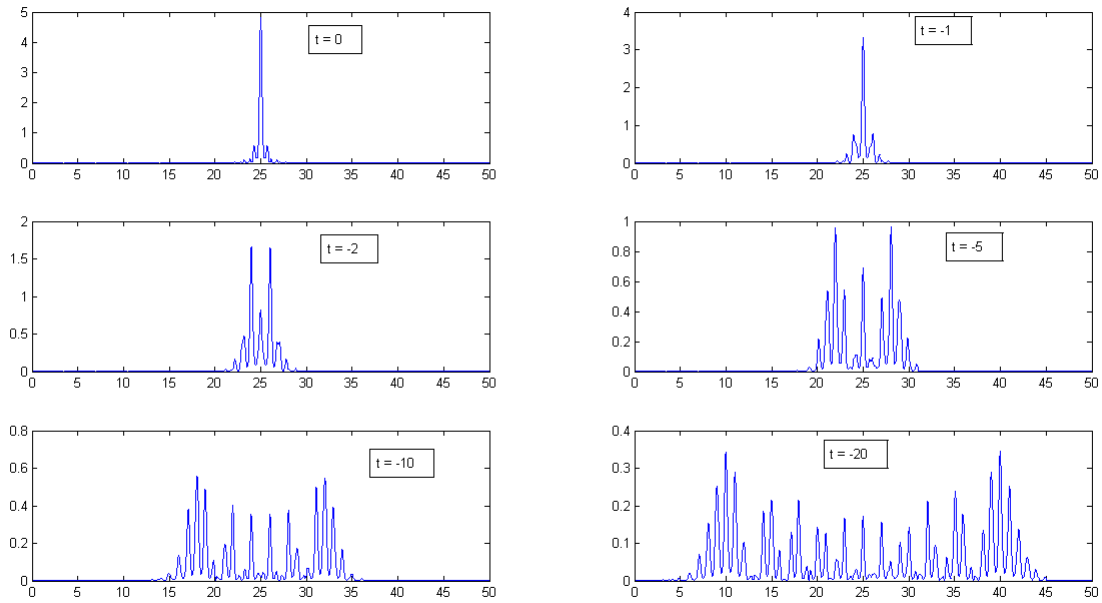

Figure 5.2: $G_0(x, x', t)$ for a fixed x' and different times

them using the simplistic model of $\delta-$functions:

$$\begin{aligned} V_{klmn} &= \int dx \int dx' \psi_k^*(x)\psi_l^*(x')V_{int}\delta(x-x')\psi_m(x)\psi_n(x') \\ &= V_{int}\int dx\, \psi_k^*(x)\psi_l^*(x)\psi_m(x)\psi_n(x) \end{aligned} \tag{5.13}$$

Now, since $\psi_k(x) = e^{ikx}u_k(x)$, where $u_k(x)$ is a periodic function, we have that the integrand in 5.13 is $e^{i(m+n-k-l)x}$ times a periodic function. Therefore the only non zero contributions are those with $m+n-k-l = nk_L$, which means crystal momentum is conserved. We only need to compute the non zero contributions of the potential which are:

$$V_{klq} = V_{int}\int dx\, \psi_{k-q}^*(x)\psi_{l+q}^*(x)\psi_k(x)\psi_l(x) \tag{5.14}$$

Where $k-q$ and $l+q$ may have to be transferred to the First Brilluin zone. This potential is so simplistic that the energy corrections predicted by the Hartree-Fock and by the ladder approximation are both zero. This is due to the fact that $V_{klkl} = V_{kllk}$ which is clear from 5.13, or, in three index notation $V_{kl0} = V_{kl(k-l)}$. Therefore we will need some model in which these two matrix elements do not cancel eachother. However this potential shares some features with the not so simplistic soft sphere potential: the computation shows that all the matrix elements such that $k-q$ and $l+q$ lie in the First Brilluin zone are of the same magnitude (for the case with $N = 10$ pairs of electrons this is in the interval $[0.13V_0, 0.17V_0]$), and those such that $k-q$ or $l+q$ do not lie in the First Brilluin zone are roughly one third of the first

ones. According to this, the approximation made in the RPA approximation, $V_{klq} \approx V_q$ is not very accurate since half of the matrix elements are one third of the other half, however we will still make use of it. The hard sphere potential is defined as $V_{HS}(x) = V_{int}$ when $|x| < r_0$ and $V_{HS}(x) = 0$ otherwise, where we use the same letter V_{int} as in the delta potential, but it should not cause confusion. We will fix $r_0 = 0.1d$, where d is the length between sites in the optical lattice. We calculated the matrix elements:

$$V_{klq} = \int\int dx dx' \psi^\dagger_{k-q}(x)\psi^\dagger_{l+q}(x')V_{HS}(x-x')\psi^\dagger_k(x)\psi^\dagger_l(x') \tag{5.15}$$

And next we computed the energy corrections using the formulas deduced in Chapter 4. Next, we will show some plots of the energy correction for the leftmost particle in the Brilluin zone. The x axis is proportional to the potential interaction V_{int}, and the y axis is the energy correction, this is shown in Figure 5.3. This first calculation is done with an optical potential depth of $V_L = 10E_r$.

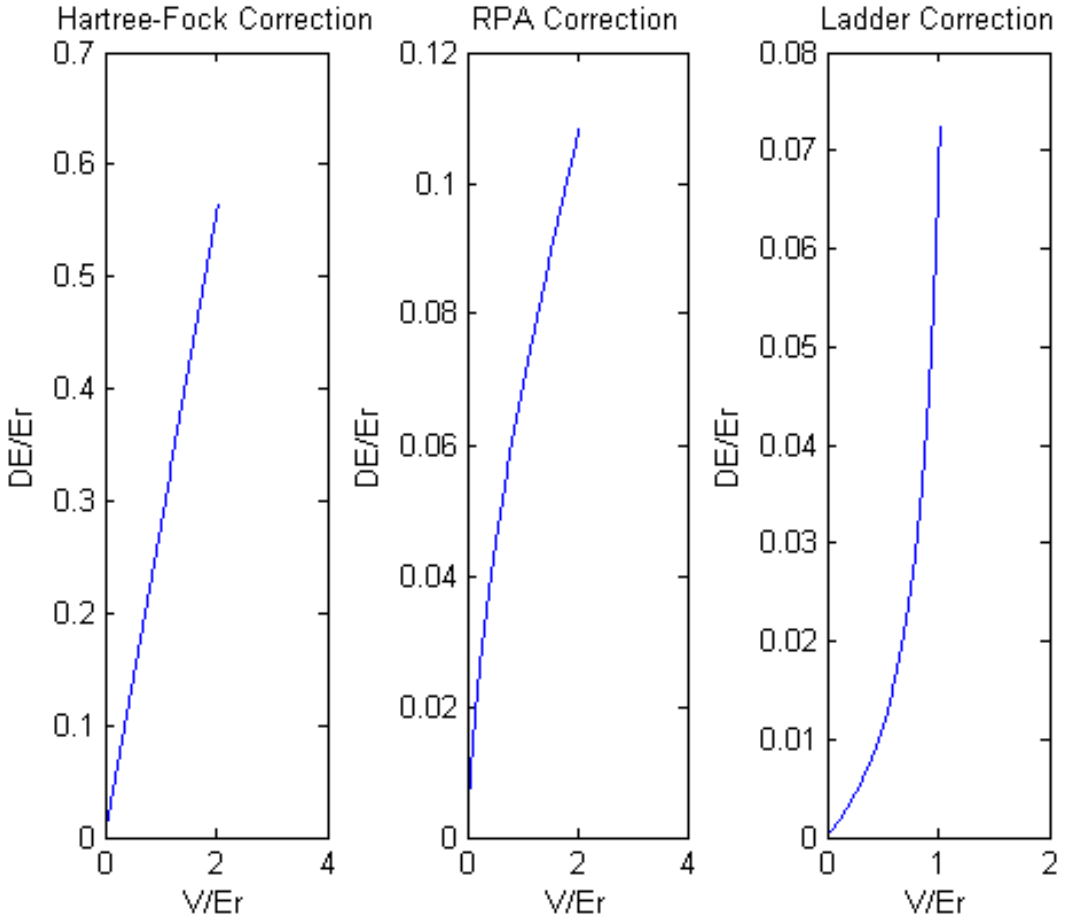

Figure 5.3: Correction energy for a soft sphere potential of radius $r = 0.1d$. Optical lattice depth $V_L = 10E_r$

Observe that all three approximations lead to different corrections in the energy, being the Hartree-Fock correction much greater than the RPA and ladder corrections. One can argue that the ladder approximation is the most accurate, since it is a good approximation for the low density/short range interaction limit. Here the average distance between particles

is d, and the range of interaction is $r_0 = 0.1d$, therefore the condition of validity of the approximation: $r_0/d << 1$ is fulfilled. On the other hand, the RPA approximation is a good approximation in the high density limit, and Hartree-Fock is a more simplistic approximation which doesn't take into account correlation effects. Next we plot the same corrections but changing $r_0 = 0.5d$, the radius of the soft sphere of the interaction potential, we obtained Figure 5.4.

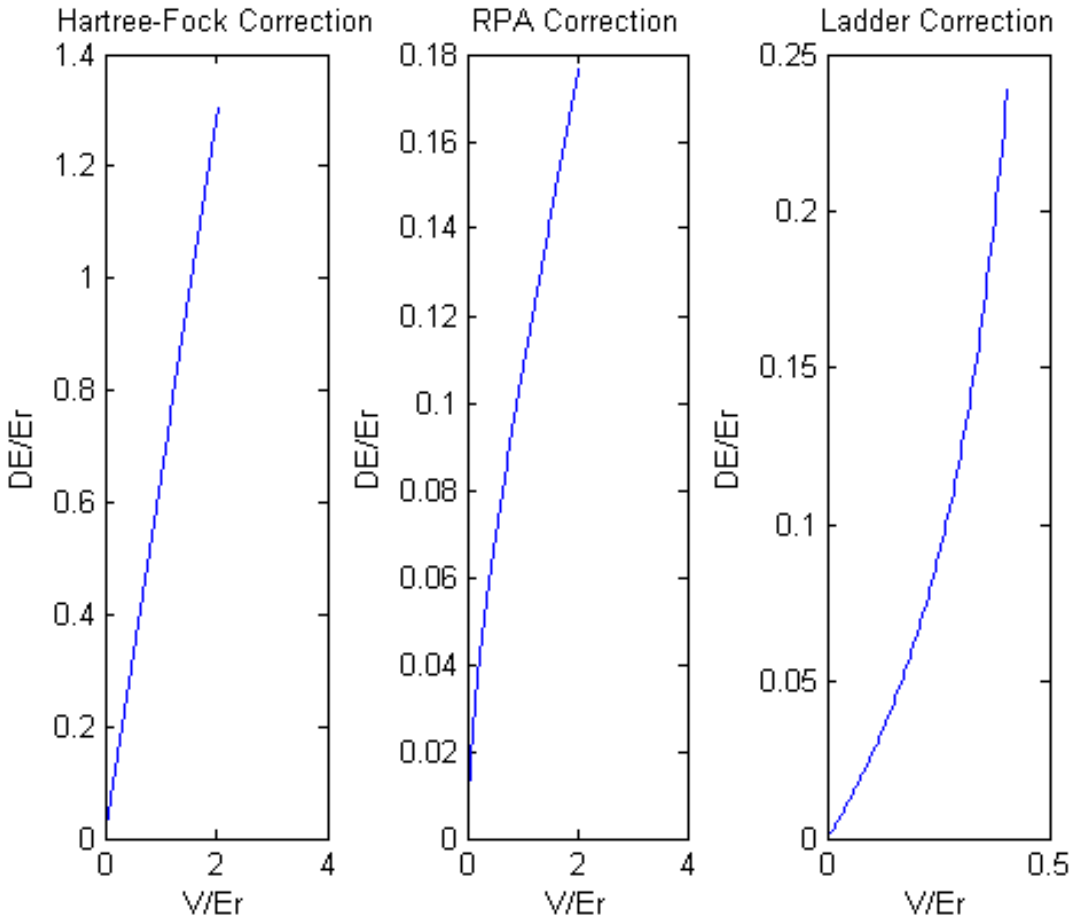

Figure 5.4: Correction energy for a soft sphere potential of radius $r = 0.5d$. Optical lattice depth $V_L = 10E_r$

As expected, the overall result is an increase of the energy correction in the three approximations. However, the increase in the ladder approximation is much greater than in the RPA and Hartree-Fock approximations. Observe that in this case we could only compute for the ladder approximation until $V = 0.2E_r$. That is because for larger values there is no convergence in the series of 4.43 so the result is meaningless.

Now we change the optical potential depth to $V_L = 5E_r$ and to $V_L = 2E_r$ and do the same calculations as before. The correction energy for this case is shown in Figures 5.5 and 5.6

Observe that the energy correction in all three approximations decreases when the potential depth is decreased from $V_L = 10E_r$ to $V_L = 5E_r$ and from $V_L = 5E_r$ to $V_L = 2E_r$. However, when the energy correction of the RPA approximation in the $V_L = 2E_r$ simulation is greater than that of the $V_L = 5E_r$ simulation. Moreover we observe a change in the convexity of the curve. We ignore the physical meaning of this.

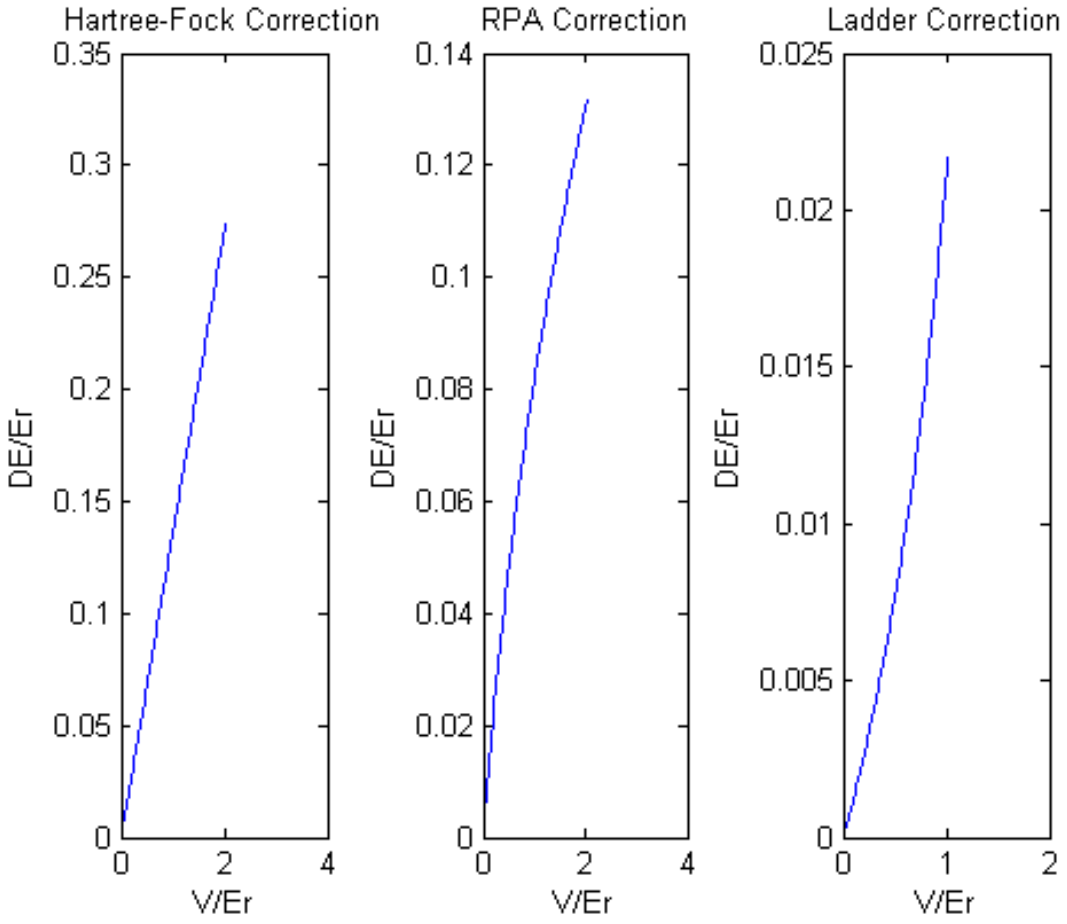

Figure 5.5: Correction energy for a soft sphere potential of radius $r = 0.1d$. Optical lattice depth $V_L = 5E_r$

We will now show the results when the Calogero-Sutherland potential is used:

$$V(x) = V_{int} \frac{\pi^2/L^2}{\sin\left(\frac{\pi}{L}x\right)} \tag{5.16}$$

This potential describes a system of particles in a ring with a Coulomb-type interaction. This is not the case of an optical lattice, but we can obtain the results anyway. We can estimate the range of this interaction as the distance at which $V_{CS}(x) = V_{SS}(0)$, that is, the point at which the Calogero-Sutherland potential equals V_{int}. That is:

$$\frac{\pi^2/L^2}{\sin\left(\frac{\pi}{L}x\right)} = 1 \tag{5.17}$$

This can be solved for $L = 10$ yielding $x_{CS} = 0.9626d$, that is, the range of the interaction is in the limit of validity of the ladder model.

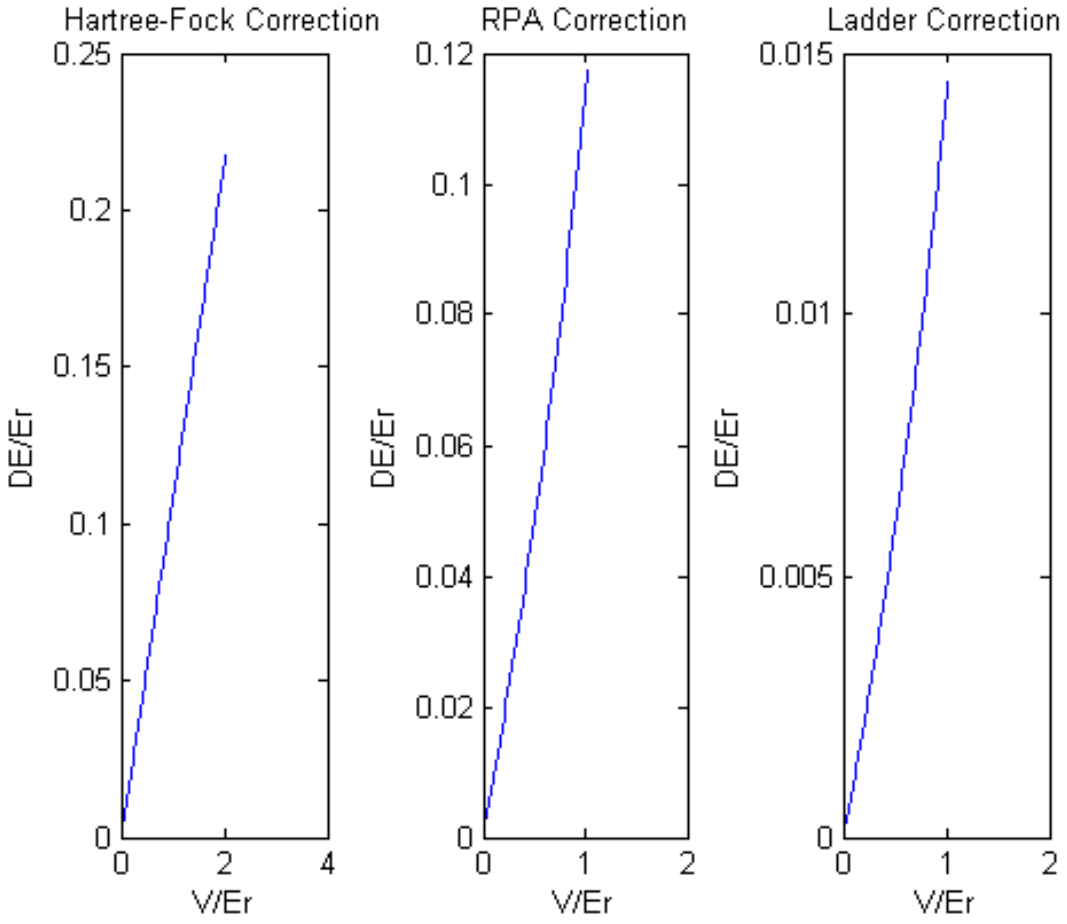

Figure 5.6: Correction energy for a soft sphere potential of radius $r = 0.1d$. Optical lattice depth $V_L = 2E_r$

First we show the correction energy for an optical lattice of depth $V_L = 10E_r$ in Figure 5.7. Observe that the values of the coupling constant are much little than in the soft spheres potential. This is because the RPA and ladder approximation diverge faster because the interaction is greater.

Observe that the resulting correction is similar to that of Figure 5.8, for which we used a soft sphere potential with $r_0 = 0.5d$. In both triplets of graphics one can see that the RPA approximation lead to a smaller correction than the Hartree-Fock and the ladder approximations. This region with $r_0 \approx d$ is the limit of validity of Hartree-Fock approximation, therefore we can expect the RPA approximation to be more accurate. Next, we change the optical potential depth to $V_L = 5E_r$ and $V_L = 2E_r$, the results are shown in Figures 5.8 and 5.9.

Observe that as we low down the optical potential V_L, the Hartree-Fock and ladder approximation lead to a decrease in the energy correction of the particles. However, the RPA approximation shows the opposite behaviour: the energy correction increases. Moreover, as in the case of the soft spheres potential, the correction curve predicted by the RPA approximation changes form concave to convex as we change $V_L = 5E_r$ to $V_L = 2E_r$.

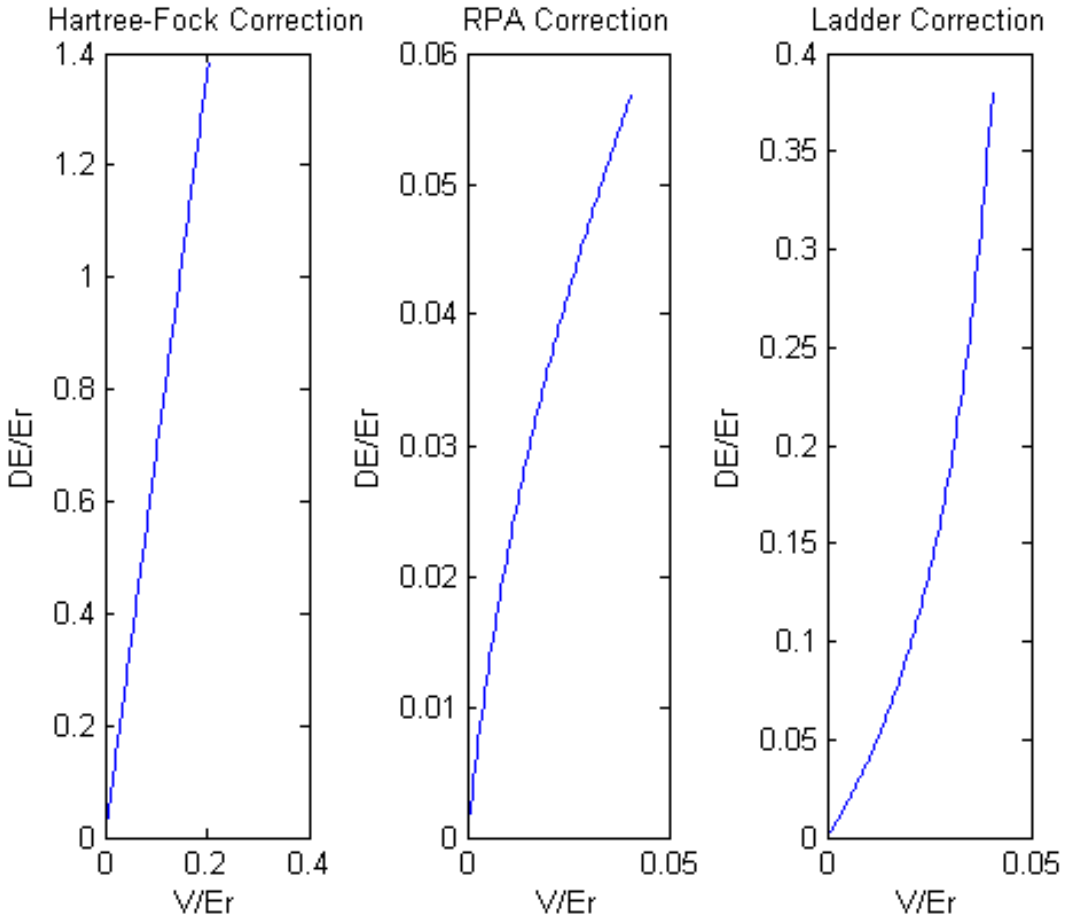

Figure 5.7: Correction energy for a Calogero-Sutherland potential. Optical lattice depth $V_L = 10E_r$

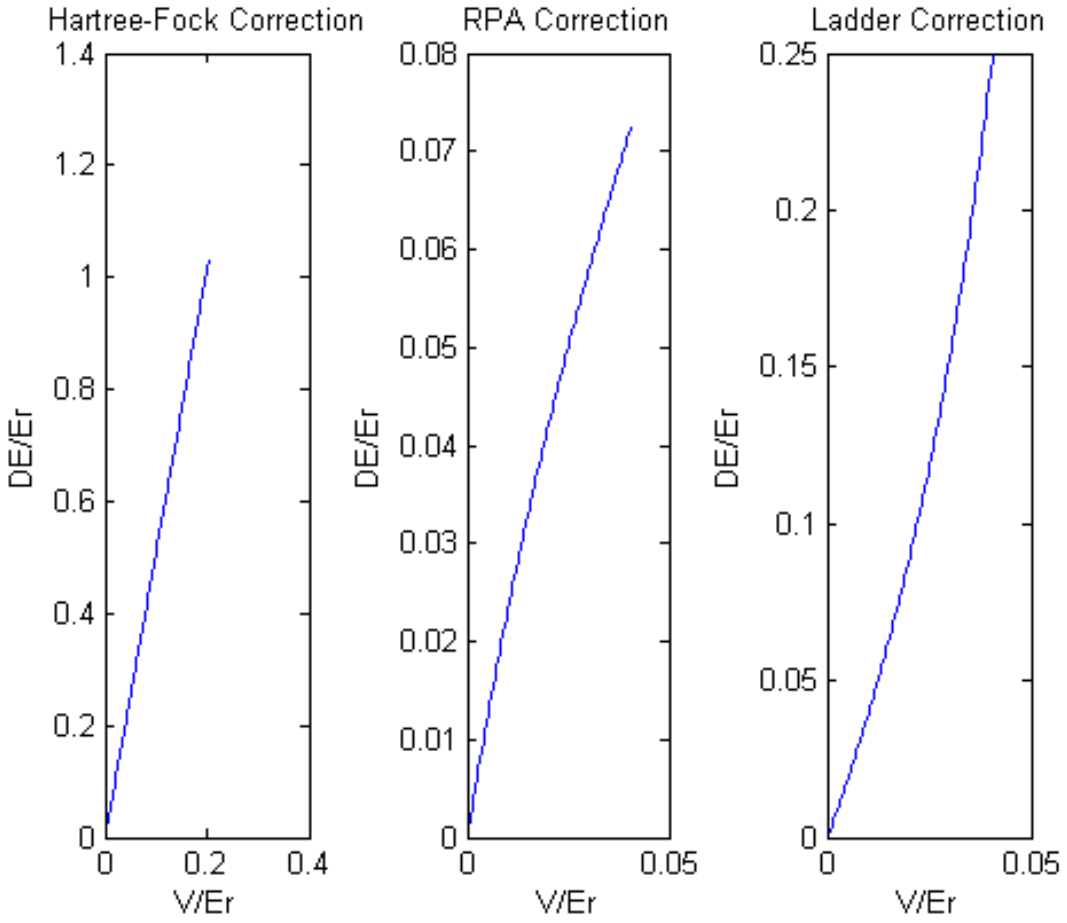

Figure 5.8: Correction energy for a Calogero-Sutherland potential. Optical lattice depth $V_L = 5E_r$

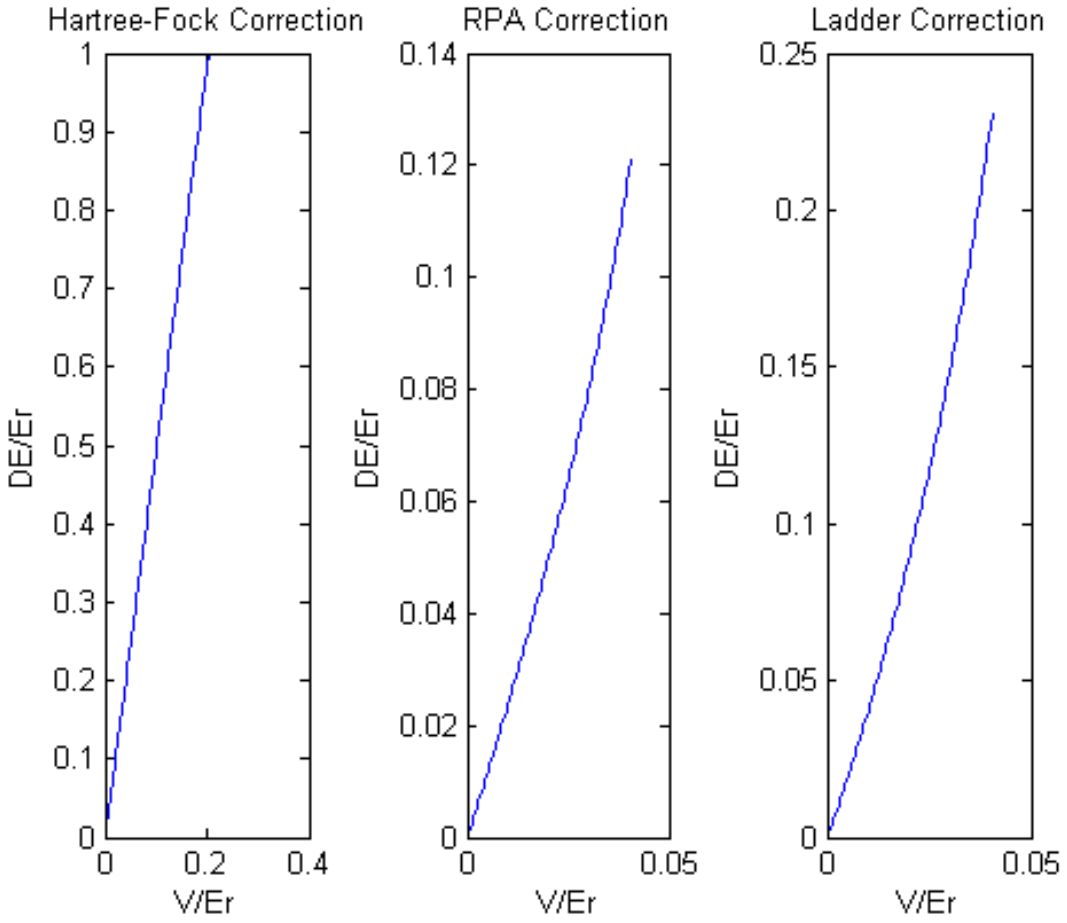

Figure 5.9: Correction energy for a Calogero-Sutherland potential. Optical lattice depth $V_L = 2E_r$

Conclusions

In this work we computed the quasi-particle energy correction for a system of interacting electrons in an optical lattice. The main purpose of this work was to study in detail the perturbative technique of Feynman Diagrams.

Although at the begging of this work we employed a Hubbard model, we decided to take first quantized toy potentials (soft spheres, and Calogero-Sutherland) and second quantize them to write down the diagrammatic expansions. Taking directly the second quantized potential of the Hubbard model was also considered. And, although it is possible, it seemed formally more complicated and less general than the approach we took.

Solid State theory was employed to obtain the solutions in the non-interacting problem. Then, we analyzed the free Green's function, which would become the pillar to write the diagrammatic expansions. Different well-known approximations of the self-energy were used to obtain the energy corrections. Some of this approximations work better than others in some cases, we tried establish which approximation should be the most accurate in the different regimes we worked.

Bibliography

[1] Alexander L. Fetter and John Dirk Walecka *Quantum Theory of Many-Particle Systems.* McGraw-Hill Book Company, 1971

[2] Richard D. Mattuck *A guide to Feynman Diagrams in the Many-Body Problem* McGraw-Hill Book Company, 1967

[3] E. K. U. Gross, E. Runge and O. Heinonen *Many-Particle Theory* World Scientific Publishing

[4] Willem H. Dickhoff and Dimitri Van Neck *Many-Body Theory Exposed! Propagator description of quantum mechanics in many-body systems* World Scientific

[5] Ashcroft and Mermin *Solid State Physics* Saunders College Publishing

[6] Maciej Lewenstein, Anna Sanpera and Verònica Ahufinger *Ultracold Atoms in Optical Lattices* Oxford University Press

[7] G. E. Astrakharchik, D. M. Gangardt, Yu. E. Lozovik and I. A. Sorokin *Off-diagonal correlations of the Calogero-Sutherland model* PHYSICAL REVIEW E 74, 021105 2006

[8] F. Calogero *Ground State of a one-dimensional N-Body System* Journal of Mathematical Physics, Volume 10, number 12, December 1969.

[9] Francesco Calogero *Calogero-Moser system* Scholarpedia(2008), 3(8):7216.

[10] Bill. Sutherland *Quantum Many-Body Problem in One Dimension: Ground State* J. Mathematical physics, v. 12, n. 2, 1971

[11] Konstantin V. Krutitsky *Ultracold bosons with short-range interaction in regular optical lattices* Physics Reports, January 14, 2015

[12] F. H. L. Essler, H. Frahm, F. Gohmann, A. Klumper, V. E. Korepin *The one-dimensional Hubbard model* December 2003

[13] R. Shankar *Principles of Quantum Mechanics* 2nd Edition, Springer

[14] C. Cohen-Tannoudji *Quantum Mechanics* Wiley; 1st edition (January 8, 1991)

[15] A. Zee *Quantum Fiel Theory in a Nutshell* 2nd Edition, Levant Books

[16] Immanuel Bloch *Ultracold quantum gases in optical lattices* Nature Physics 1, 23 - 30 (2005)

[17] Matthias Ohliger and Axel Pelster *Greens Function Approach to the Bose-Hubbard Model* World Journal of Condensed Matter Physics, 2013, 3, 125-130

[18] *The Hubbard model at half a century* Nature Physics 9, 523 (2013)

[19] Joshua Ellis *TikZ-Feynman: Feynman diagrams with TikZ* arXiv: 1601.05437 [hep-ph]